Soft Matter

Cite this: *Soft Matter*, 2012, **8**, 3683

www.rsc.org/softmatter

PAPER

Probing the dynamics of particles in an aging dispersion using diffusing wave spectroscopy

Jérôme Crassous* and Arnaud Saint-Jalmes

Received 6th March 2012, Accepted 12th May 2012
DOI: 10.1039/c2sm25526j

We have studied theoretically and experimentally the dynamic multiple light scattering properties of a liquid dispersion (an aqueous foam for the experiments) having a continuous phase doped with colloidal scatterers (monodisperse latex beads for the experiments). The temporal auto-correlation function of the scattering intensity shows two characteristic timescales. The slow timescale is related to the reorganization of the dispersion induced by aging, while the fast timescale is related to the Brownian dynamic of the colloids. Although the static light scattering properties are fully controlled by the dispersion at a large scale, the dynamic scattering is surprisingly highly sensitive to even a tiny amount of added colloids. The non-trivial generic behavior discussed here reveals that using multiple light scattering to study complex and real industrial or food-related dispersed products requires special care to avoid possible misinterpretations.

I. Introduction

A remarkable feature of a large range of soft matter materials is that they age: colloidal suspensions and glasses, dispersed systems (like foams and emulsions), gels, pastes, *etc.* are out-of-equilibrium systems and evolve generally irreversibly with time.[1] To fully understand these soft matter systems – together with structural studies – one needs to elucidate how the supramolecular arrangements and mesoscopic organization evolve in time, and what are the intrinsic dynamical processes.

As many of these systems are opaque, it is not straightforward to visualize and monitor internal dynamics. An optical technique based on the diffusive walk of photons inside the material – Diffusing Wave Spectroscopy (DWS) – emerged in the early 90s.[2–5] The first DWS results, mostly on model systems like colloidal solutions of polyballs and commercial foams,[3,6–8] rapidly proved that DWS is a powerful tool for investigating dynamics in turbid media. Over the years, advances and refinements were made on both the theoretical[9,10] and technical aspects. In particular, improvements were made to tackle statistically non-trivial dynamics and ergodicity issues: developments of multi-speckle[11] and double cell setups,[12] and advanced DWS-inspired techniques like speckle visible spectroscopy[13] and time-resolved correlation.[14]

The natural aging of the materials is not the only source of internal dynamics; applying a shear can also lead to microscopic rearrangements, and DWS can monitor these rates of shear-induced motions, and more generally the balance between aging and shear.[6,15–21] In that respect, as DWS is a measurement at a local microscopic scale, it also offers microscopic interpretation of macroscopic rheology, allowing us to draw the complex links between micro- and macroscopic features.

In the last ten years, DWS has also emerged in food science,[22–24] as more and more correlations were drawn between food samples and other soft materials.[25] However, food systems are generally much more complex, both in terms of chemical formulation and processes, than model systems studied initially by DWS. Indeed, food samples typically comprise complex fluids, already often opaque and containing their own light scatterers (like casein micelles, oil droplets, protein aggregates and coacervates, and surfactant–polyelectrolyte complexes). These fluids are then mixed, embedded into out-of-equilibrium jellified matrices, or distributed into multiple dispersions. Along with the complexity of the formulation and structure, these systems evolve under various dynamical processes: beside their own aging, changes are often induced by varying the external conditions (like pH, temperature or applied stress), leading to macroscopic features like gelification, coagulation, destabilization, or flocculation.[26–32]

In such systems, because of multiple interactions and components, it is far from simple to determine what is the source of the photon decorrelation, and to ascribe the timescale extracted from the DWS data to the relevant mechanism. Understanding DWS data in real complex formulations and structures – such as those found in food applications – remains a challenging issue, and these aspects are indeed the less investigated and understood situations. In other words, the tricky task is not to perform a DWS measurement, but to determine what the DWS curve actually reports, when dealing with non-trivial multiple component/scatterer systems dispersed one into

Institut de Physique de Rennes, UMR 6251 CNRS/Université Rennes 1, Campus Beaulieu, Bâtiment 11A, 35042 Rennes Cedex, France. E-mail: jerome.crassous@univ-rennes1.fr

another. At this stage, the first important step is to better understand what is measured by DWS in systems of moderate and controlled complexity.

In that respect, while studying the properties of a new class of aqueous foams, namely those solely stabilized by nanoparticles (like the more classical Pickering emulsions[33,34]), we performed DWS measurements on such foams.[35] Unusual features were observed: inspired by a previous work on packed solid particles,[36] it was proposed that these results could be due to a tiny amount of remaining free floating particles (those not adsorbed at interfaces). But only partial analysis and hypothesis verifications could be done. Indeed, too many unknown parameters were involved with these particle-stabilized foams: the shape and size of the particles (probably aggregated in clogs), the actual concentrations of non-adsorbed particles, technical issues on the foam production leading to uncontrolled foams, and uncontrolled slow aging dynamics (mostly film ruptures leading to uncontrolled bubble size and polydispersity). Thus the whole interpretation framework could not be validated, and limits of our models could not be identified. These first experiments were more like a proof of concept where, when dealing with mixtures of scatterers, new features occur.

To elucidate in detail the situation where small scatterers and large globules (like oil droplets or gas bubbles) are dispersed together in water, we experimentally investigate here a typical case of this class of system. We choose to study foams doped with colloidal particles and focus particularly on the regime of low concentrations of added particles, which turns out to be both theoretically and experimentally (for applications) the most interesting. This new quantitative DWS study shows that it is possible to separate the intrinsic dynamics of the foam and of the particles, only for a range of relative concentrations, unexpectedly corresponding to the limit of very low concentrations of colloids. In parallel, we present a theoretical formalism for DWS corresponding to the general case of small and rapid colloidal scatterers in an aging dispersion matrix, and compare the predictions to the data, and discuss the limits of the model.

II. Theoretical background: the general case of colloidal scatterers within a liquid dispersion

For the theoretical modeling, we consider a system as generic as possible: as depicted schematically in Fig. 1a, it consists of a liquid dispersion (being a foam or an emulsion) where the dispersed globules (respectively bubbles or droplets) are of typical diameters larger than 10 μm. We do not make a restrictive hypothesis on the size distribution of the globules. Inside the continuous phase of this dispersion, a small amount of free colloidal particles is also dispersed. The diameter of the colloidal particles is supposed to be small compared to globules and to the inter-distance between globules, so that colloids diffuse freely in the continuous phase. Although we carried out experiments and modelling only with calibrated beads, generalization to polydisperse systems may be easily considered.

This dispersed system is then illuminated with a coherent light (wavelength inside the material λ), and we consider, as depicted in Fig. 1b, a path of length, s, inside the dispersion. We draw on the figure a slab geometry in transmission, but other geometries

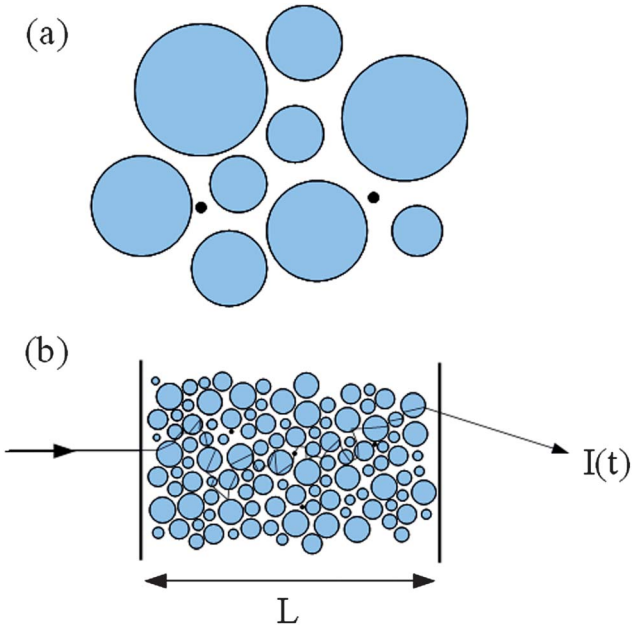

Fig. 1 (a) A schematic view of the generic system discussed theoretically: large globules (oil droplets or gas bubbles, in blue on the figure) of typical size >10 μm with few colloidal scatterers (black points on the figure). (b) A schematic drawing of the slab geometry that we used for the DWS study, with the path for one photon.

may also be considered. We call $\Delta\Phi_s(t, t+\tau)$ the variation of the phase $\Phi_s = ks$ between the time t and $t+\tau$, with $k = 2\pi/\lambda$. We consider also that the dispersion system strongly scatters light, *i.e.* the transport mean length of the system l^* is small compared to the material size. Typically for liquid dispersions (foam or emulsion), the transport mean free path is a few globule (bubbles or droplets) diameters.

In the following, we consider that the dynamics of our system is twofold. First, there is a slow aging of the dispersion, leading to globule reorganization. Those reorganizations create important phase variations for paths where reorganization occurs. We suppose that reorganizations of the dispersion occur into the bulk sample with a constant probability per unit of volume and unit of time. So the probability that a reorganization occurs for a path of length s during a time interval τ is $p_R = 1 - \exp(-s\tau A)$, with A being a constant depending on the bulk properties of the dispersion. It is interesting to introduce the characteristic time $\tau_R = 1/Al^*$, which is the characteristic time between two reorganization events occurring on a path of length l^*. The value of the phase variation for paths where at least one reorganization occurs is $\Delta\Phi_s(t, t+\tau) = r$, with r being a random number. Since the reorganization occurs for a typical size of a few droplets or bubbles which is, by hypothesis, at least 10 μm, the path length variations are expected to be large compared to the optical wavelength, and $|r| \gg 2\pi$.

The second dynamical contribution leading to light path changes is the motion of the colloidal particles dispersed into the continuous fluid. For a path with no globule reorganization, we call l_c the mean distance between two scattering events by small particles. We suppose that those colloidal particles are distributed randomly into one phase of the emulsion; the probability

that n scattering events occur for a path of length s should follow a Poisson distribution $p_n(s) = \mu^n \exp(-\mu)/n!$, with $\mu = s/l_c$. The phase shift for one path with n scattering events is $\Delta\Phi_s(t, t+\tau) = \sum_{i=1}^{n} \boldsymbol{q}_i \cdot \Delta\boldsymbol{r}_i(t, t+\tau)$ with $\boldsymbol{q}_i$ being the scattering vector of the i^{th} scattering event, and $\Delta\boldsymbol{r}_i(\tau)$ being the displacement of the i^{th} scatterer. The probability that n scattering events occur without globule reorganization is $(1 - p_R)p_n$.

The correlation function $g_E^{(s)}(\tau) = \langle \boldsymbol{E}(t) \cdot \boldsymbol{E}^*(t+\tau) \rangle$ of the scattered electric field for path of length s may be written as:

$$g_E^{(s)}(\tau) = \sum_{n=0}^{\infty} p_n \left\langle \exp\left(j \sum_{i=1}^{n} \boldsymbol{q}_i \cdot \Delta\boldsymbol{r}_i(t, t+\tau) \right) \right\rangle \times [(1 - p_R) + p_R \langle \exp(jr) \rangle] \quad (1)$$

$$= (1 - p_R) \sum_{n=0}^{\infty} p_n \langle \exp(\boldsymbol{q} \cdot \Delta\boldsymbol{r}(\tau)) \rangle^n \quad (2)$$

The first term in eqn (1) is a summation of a path which contains no reorganization, and the second term is the summation of a path that contains reorganization, and also possibly scattering with colloidal particles. In eqn (1) averages are calculated for different paths, scattering events, and reorganizations. For obtaining eqn (2) we used the fact that the different scattering events are independent, and that $\langle \exp(jr) \rangle = 0$ because r is a random variable with $|r| \gg 2\pi$. The average in eqn (1) is calculated for all scattering vectors for scattering events with small particles. We note $g_E^{(B)}(\tau) = \langle \exp(\boldsymbol{q} \cdot \Delta\boldsymbol{r}(\tau)) \rangle$ the correlation function for a single scattering on a colloidal particle. Replacing p_R and p_n by their expressions, and after a little calculation we find:

$$g_E^{(s)}(\tau) = \exp\left[-\frac{s\tau}{l^* \tau_R} - \frac{s}{l_c}\left(1 - g_E^{(B)}(\tau)\right) \right] \quad (3)$$

The correlation function for a distribution $P(s)$ of path lengths is $g_E(\tau) = \int P(s) g_E^{(s)}(\tau) \mathrm{d}s$. Rewriting eqn (3) as $f(\kappa) = \exp(-\kappa s)$ with $\kappa = (\tau/l^*\tau_R) + (1 - g_E^{(B)}(\tau))/l_c$, we have $g_E(\tau) = \int P(s) \exp(-\kappa s) \mathrm{d}s$. For the sake of simplicity, we restrict to the situation of a parallel slab of thickness $L \gg l^*$ in the transmission geometry, but results may be easily extended to other scattering geometries. In this case, the Laplace transform of $P(s)$ may be computed analytically[4] and is approximately $g_E(\tau) \simeq \exp(-\kappa L^2/2l^*)$. Then eqn (3) becomes:

$$g_E(\tau) \simeq \exp\left[-\frac{L^2\tau}{2(l^*)^2\tau_R} - \frac{L^2}{2l^* l_c}\left(1 - g_E^{(B)}(\tau)\right) \right] \quad (4)$$

Expression (4) in the limit case $\tau_R \to \infty$ is analogous to expressions calculated for Brownian particles dispersed in porous materials,[4,36,37] where reorganizations are absent. Taking into account such reorganizations adds a decay of the correlation on a time scaling with τ_R, and depending on the geometrical and optical parameter l^* and L.

Lastly, the function $g_E^{(B)}(\tau) = \langle \exp(\boldsymbol{q} \cdot \Delta\boldsymbol{r}(\tau)) \rangle$ may be calculated for point like scatterers, and it has been found that:[37,38]

$$g_E^{(B)} = \left[1 - \exp(-\tau/\tau_B)\right] \tau_B/\tau \quad (5)$$

with $\tau_B = 1/4k^2D$, where D is the Brownian diffusion coefficient of the colloidal particles.

III. Model experimental system: latex beads within a foam

The experimental system we selected to investigate the scattering properties of such composite materials and to test the previous model is an aqueous foam doped with latex beads.

More precisely, we chose to perform experiments with a commercial shaving foam (from Gillette); such shaving foams have been used to tackle various issues of the physics of foams (for instance, for optics or mechanics[7,19,20,39,40]). The major advantage of shaving foams is that all of them share the same reproducible initial and aging properties, independent of the exact chemical formulation. Indeed, for all basic shaving foams, the initial liquid fraction is typically $\varepsilon_l \simeq 7\%$. The initial mean bubble size is typically $\sim$40 μm at the foam fabrication $t = 0$. All these foams have similar bubble size polydispersity and high uniformity (no holes or voids). They are also very robust against bubble coalescence. As a consequence of the small initial value of the bubble diameter, such foams evolve in time mostly by coarsening (due to gas diffusion), almost without drainage or coalescence.[41] Quantitatively, the bubble diameter increases by a factor 8–10 in 1000 minutes, while drainage makes the liquid fraction decrease by less than 15% over that timescale; moreover, drainage is basically stopped when using samples of typically a few cm of height (as used here) due to the liquid capillary holdup. Note that this coarsening is a self-similar process and the bubble diameter evolves as $\sqrt{t}$.[7,8] More importantly, bubble rearrangements are induced by this coarsening process, and it has been reported that the reorganization timescale varies as $\tau_R \sim t^{2.0}$ and is typically of the order of 1 s.[7,8] Therefore, using shaving cans is a simple and efficient way to reproducibly obtain controlled samples belonging to the same class of foams, meaning those with low liquid fraction, tiny bubble size, strong stability and a slow and simple aging (solely dominated by coarsening).

For the colloidal particles, monodisperse polystyrene latex beads are purchased from Sigma-Aldrich (named *LB-1* for 100 nm diameters and *LB-3* for 300 nm diameters). The particles are used as received, dispersed into a surfactant solution (to prevent destabilization in time), and at a solid volume fraction of 10%.

To prepare the samples, a mass $\sim$500 mg of foam is weighed, and a controlled volume of the latex beads solution is added to the foam. We define the volume colloidal fractions Φ_c as the volume of colloidal particles over the volume of the foam (constant over time, as well as the volume of the liquid inside the foam). The mixture is gently stirred for one minute. We have checked that the same stirring procedure with ink instead of colloidal suspension ensures a homogeneous dispersion of the added liquid inside the foam. We have also checked that previous dilution of the colloidal suspension prior to mixing with the foam does not change results. Note that such a mixing method was also used previously with particles of tens of microns and commercial foams to study rheological behavior.[42]

The presence of the colloidal particles does not modify the foam stability and aging. No differences have been found by visual inspections over a few hours when comparing a foam with and without added particles. In parallel, adsorption of some particles at the interfaces is not expected, because of the negative charge of the particles, their high hydrophilicity and the slow stirring protocol used here.[43]

In practice, we have thus various experimental adjustable parameters: the particle size, the amount of particles (measured by the volume colloidal fractions Φ_c) and the foam age, which means various bubble diameters.

The mixture of foam with colloidal particles is then put into a cell with two parallel glass plates separated by $L = 4.0$ mm (Fig. 1b). A laser beam (He–Ne, 633 nm, 5 mW) is expanded with a lens to illuminate the entire cell. The scattered light is observed in transmission and is collected with a single-mode optical fiber with a collimation optic. The fiber output is sent on a photomultiplier, and the normalized intensity auto-correlation function $g_I(\tau) = \langle I(t)I(t+\tau)\rangle/\langle I(t)\rangle\langle I(t+\tau)\rangle$, with $\langle\cdot\rangle$ being a time average, is measured with a digital correlator (Flex02-12D from correlator.com) operating in multi-tau mode. The typical photon rate is ~10 kHz, and correlation functions are obtained after 10 min averages.

IV. DWS data and dependence on the system parameters

Fig. 2a compares the raw correlation functions obtained for a foam without colloidal particles, and foams with free different amounts of added colloidal particles, the aging time and the particle diameter being the same. The intercept $g_I(\tau \to 0)$ is always close to 1.5 which is the expected theoretical value for an unpolarized scattered wave.[44] Without colloidal particles, we find a decay of correlation on a typical timescale of ~0.1 s as commonly reported.[7,8] The effect of adding colloidal particles is to add a "fast" decay on a timescale $\tau \simeq$ ms to the correlation function. The amplitude of the first decay is clearly related to the amount of colloidal particles introduced into the foam.

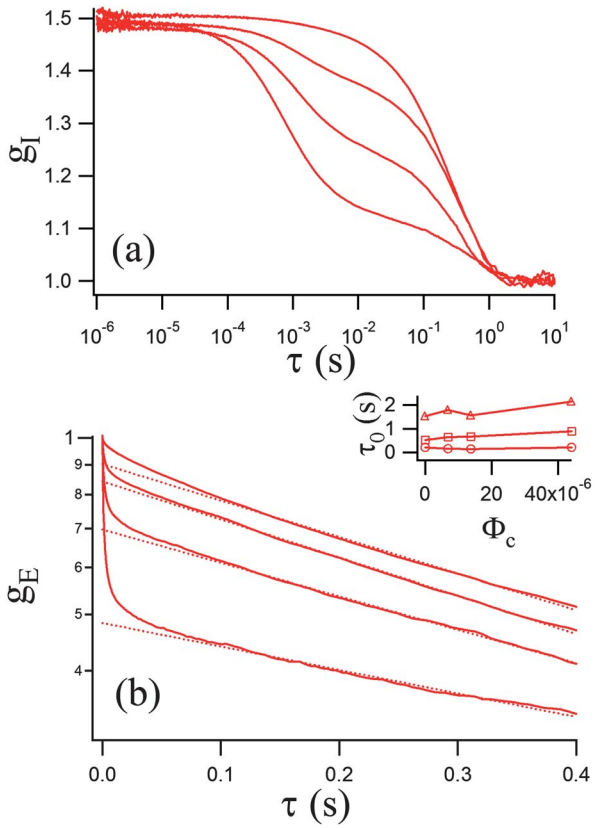

Fig. 2 (a) Raw data g_I *versus* delay τ in a lin–log plot. Top curve is foam only, and the solid fraction of latex sphere ($d = 300$ nm) increases from the top to bottom curve $\Phi_c = 6.92 \times 10^{-5}$; 13.8×10^{-5} and 44.1×10^{-5}. The foam age is $t \simeq 620$ min for every foam. (b) g_E *versus* τ for the same data in a log–lin scale. Plain lines are experimental data and dotted lines are exponential fit $g_E(\tau) = g_E^* \exp(-\tau/\tau_0)$ for $\tau \geq 0.1$ s, with g_E^* and τ_0 two fitting parameters. Inset: τ_0 as a function of Φ_c for $t = 100$ min (○) $t = 500$ min (□), and $t = 1000$ min (△).

By contrast, the "slow" decay time is unaffected by the presence of the colloidal particles, and can be unambiguously ascribed to the coarsening of the foam (as $\tau \sim s$ and by similarities with previous studies).

At lower concentrations, no effects are observed (only a single decay due to the foam coarsening dynamics); but for concentrations of the order of 10^{-3}, one can also measure a single decay, but linked to the particles dynamics, and fully hiding the slow one of the foam. We emphasize that between these two situations, leading to the same qualitative shape of the DWS curve, there is a difference of typically 3 orders of magnitude in timescales.

As a last comment on this description of the raw data, note that all these features are robust and are observed for the different waiting times (*i.e.* different bubble diameters) and for the two particle diameters. In addition, these new results on controlled samples are in agreement with the interpretation made in a previous work.[36]

These data can also be used to determine the electric field correlation function $g_E(\tau)$, which is the quantity of interest for comparison to models, using the Siegert relation:[45] $g_1 = 1 + \beta|g_E|^2$ where β is obtained as the limit of $g_1 - 1$ for $\tau \to 0$, and where we suppose that g_E is real. The electric field correlation functions corresponding to the data of Fig. 2a are plotted in Fig. 2b.

The same features as described before are recovered in these correlation functions $g_E(\tau)$ plotted here in the log–lin scale (Fig. 2b): in the presence of colloidal particles, a two-scale decay of the correlation function for a given range of low concentrations, a first decay time independent of the concentration but an amplitude increasing with concentration, and a second decay completely independent of the added particles.

As previously noticed, we did not see any effect of added colloidal particles on the coalescence of the foam. Direct visual observations show identically stable foams. This is in agreement with the long-time decay of the correlation functions. Indeed, we did not find (see inset of Fig. 2b) any evolution of τ_0 with the amount of added colloidal particles. This indicates that the characteristic time of reorganization τ_R does not depend on the amount of colloids. We also noticed that the short decay time is independent of the amount of added particles.

In the next section, the objective is to explain these features in detail, in this well controlled setup.

V. Fitting data and discussion

We introduce τ_B the typical time of the fast decay related to the Brownian motion of the colloidal particles. We focus first on the limit $\tau \gg \tau_B$: going back to the model of Section 2, this

corresponds to $g_E^{(B)} \simeq 0$. Thus, the electric field autocorrelation function becomes:

$$g_E(\tau) \simeq \exp\left[-\frac{L^2}{2(l^*)^2}\frac{\tau}{\tau_R} - \frac{L^2}{2l^* l_c}\right] \quad (6)$$

The exponential decay of $g_E(\tau)$ is clearly visible in Fig. 2b. In this limit, for a foam at a fixed value of coarsening time and with a given solid fraction, we may fit $\ln(g_E(\tau))$ as a function of τ with an affine variation $\ln(g_E(\tau)) = \ln(g_E^*) - \tau/\tau_0$, with $g_E^* = \exp(-L^2/2l^* l_c)$ and $\tau_0 = 2(l^*)^2\tau_R/L^2$. From a practical point of view, data are fitted in the range $0.1 \leq \tau \leq 0.4$ s for $t = 500$ min, and between $0.25 \leq \tau \leq 0.5$ s for $t = 1000$ min.

The intercept g_E^* basically represents how much correlation remains after the first fast decay. To quantitatively represent the effect of the particle concentration on the decorrelation, Fig. 3 shows $-\ln(g_E^*)$ as a function of volume colloidal fractions Φ_c, as previously defined as the volume of colloidal particles over the volume of the foam, for different bead diameters and foam coarsening times.

Our model gives $-\ln(g_E^*) = L^2/2l^* l_c$ and experimentally we have found that $-\ln(g_E^*)$ increases linearly with Φ_c: this is consistent as l_c – which is the mean distance between two scattering events on colloidal particles – decreases with Φ_c.

For further analysis, we can compare the slopes of Fig. 3 to predictions, and discuss the intercept of the affine fit and the range of Φ_c corresponding to the transition range when $0 < -\ln(g_E^*) < 1$).

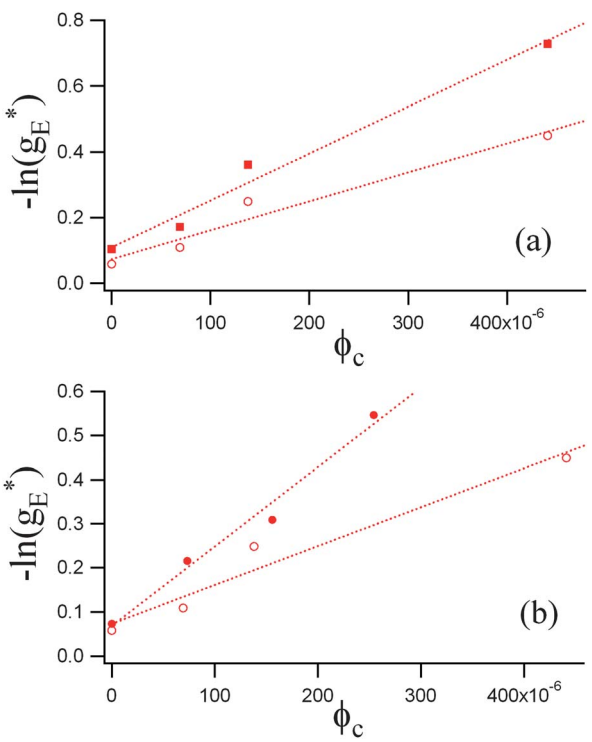

Fig. 3 Variation of the correlation drop g_E^* as a function of volume fraction of colloidal particles Φ_c into the foam. (a) Colloidal particles diameter is $d = 100$ nm and coarsening time are $t = 500$ min (■), and $t = 1000$ min (○). (b) Coarsening time is $t = 1000$ min and colloids particles diameters are $d = 100$ nm (○) and $d = 300$ nm (●). Dotted lines are affine fits of $\ln(g_E^*)$ with Φ_c.

By definition, $l_c = 1/n_c\sigma_c$, with n_c being the number of colloidal particles per unit volume and σ_c being the scattering cross-section of colloidal particles dispersed into the foam. With $n_c = 6\Phi_c/\pi d^3$, we expect $-\ln(g_E^*) = \Phi_c L^2\sigma_c/3\pi l^* d^3$. So, from the slope of the affine variations, we may obtain an estimate of $L^2\sigma_c/3\pi l^* d^3$. As expected, this slope depends on colloidal diameters (see Fig. 3b) and on foam age (see Fig. 3a) because l^* increases with the foam age. Comparison of the measured slopes $\Delta(-\ln(g_E^*))/\Delta\Phi_c$ with the expected slopes $L^2\sigma_c/3\pi l^* d^3$ is not easy, because we need values of the colloidal cross-sections σ_c. Inversely, we can estimate σ_c from the experimental data. We used reported values of variations of l^* *versus* coarsening time for Gillette foams.[8,46] We found $\sigma_c = 56$ nm^2 ($t = 500$ min, $d = 100$ nm), $\sigma_c = 55$ nm^2 ($t = 1000$ min, $d = 100$ nm) and $\sigma_c = 3040$ nm^2 ($t = 1000$ min, $d = 300$ nm). Those values may be compared, in a very crude approximation, to calculated values[47] of cross-section for Mie particles of refractive index $n_{latex} = 1.59$ dispersed in water: $\sigma_c = 57$ nm^2 for $d = 100$ nm, and $\sigma_c = 14\,900$ nm^2 for $d = 300$ nm. There is a good agreement for particles with $d = 100$ nm, confirming the whole theoretical framework leading to the predicted values of the slopes in Fig. 3. However, forcing the data for $d = 300$ nm to fit the model leads to unexpectedly low values of concentration. In the following, we show that another discrepancy, consistent with this first one, is also found for the timescale of the fast decay with $d = 300$ nm.

In the previous paragraph, we calculated l_c with the volume fraction of colloidal particles Φ_c *in the foam*. This supposes implicitly that the fraction of a photon path into the liquid is the liquid fraction. For dry foams, this assumption seems to be in qualitative agreement with the experiment.[48] Measurements of decorrelation due to colloidal particles may be used to obtain the fraction of a photon path into one phase. This is a quantity involved in the model of transport of light into a dispersed system.[49–51]

In Fig. 3, note also that there is a non-zero intercept without added particles in the limit of $\Phi_c = 0$. This may be related to the fact that we used a commercial shaving foam which is made from a solution of complex chemical formulation, and diffusive motion of pre-existing scatterers may be responsible for a small fast decay, even without added colloidal particles. Nevertheless, the effect is small and the initial foaming fluid probably contains either an extremely low amount of scatterers or scatterers with small sizes. In parallel, it should be noted that small partial decorrelation in the Gillette foam has been already reported, but this was a non-exponential contribution spanning over several decades and whose origins are different from what is discussed here (effect of thermal jittering of the bubble interfaces[15]).

Lastly in Fig. 3, we want to emphasize that the range of Φ_c which corresponds to the intermediate regime ($0 < -\ln(g_E^*) < 1$) is set, not by the scattering properties of the solution itself (l_c), but by the combination of the foam, setup and fluid properties: indeed, the important relation providing the range of Φ_c is that $L^2/l^* l_c = 1$. So, if L^2/l^* is large (up to meters), a plateau can be seen for a value of l_c of the same order of meters, meaning a very dilute and transparent solution. In that respect, these new results and analyses indeed confirm the interpretations proposed in our previous work on uncontrolled foams.

To be complete, we also have to analyze the fast decay of correlation functions due to the Brownian motion. The function

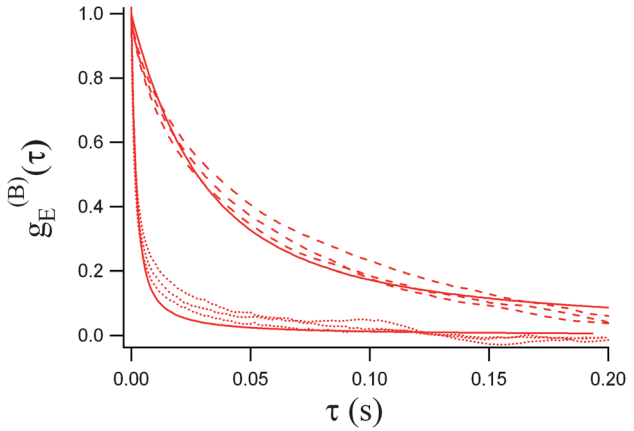

Fig. 4 Correlation functions $g_E^{(B)}$ as a function of delay τ. Dotted lines are for colloidal particles of diameter $d = 100$ nm, and dashed lines for $d = 300$ nm. The three different lines are for three different concentrations. Plain lines represent the fitting discussed in the text.

$g_E^{(B)}(\tau)$ may be extracted from experimental data as $g_E^{(B)}(\tau) = \ln(g_E/g_E^* \exp-(\tau/\tau_0))/\ln(g_E^*)$. Fig. 4 shows the extracted values of $g_E^{(B)}(\tau)$ for particle diameters $d = 100$ nm and $d = 300$ nm at different solid concentrations. One first notes that the decay of $g_E^{(B)}$ is almost independent of the colloidal solid fraction.

Plain lines correspond to the adjustment of the data by eqn (5), and we have obtained $\tau_B = 1.2$ ms for $d = 100$ nm, and $\tau_B = 18$ ms for $d = 300$ nm. In comparison with the predicted values, we use the Stokes–Einstein expression for the diffusion coefficients and taking $\eta = 1.9\ cP$ (ref. 17) for the liquid phase of the foam, this provides $\tau_B = 0.6$ ms for $d = 100$ nm and $\tau_B = 1.8$ ms for $d = 300$ nm. As for the amplitude of decorrelation, there is a reasonable agreement between experiments and the model for $d = 300$ nm, while there is one order of magnitude of difference for $d = 300$ nm.

Clearly, the model well describes the properties of the foam mixed with 100 nm diameter particles, while it fails for the 300 nm. A better agreement can be found by artificially decreasing the concentration, much smaller than what it actually is. One can then wonder if all the particles remain free in their motion. If it is clear that the liquid channel dimensions are always large enough (typically 10 microns for the internal radii) to avoid the capture of single 100 or 300 nm particles,[52] it might be possible to immobilize or reduce the motion of particles by the creation of arches and clogs and thus to effectively reduce the amount of moving particles. One might also wonder if the confinement in non-isotropic long and slender channels cannot affect the Brownian dynamics, even though the channel typical internal radius is always large when compared to the particle diameters. Another source of discrepancy, especially for the estimation of τ_B, is the point-like scatterer approximation which is probably a too crude approximation, and $\langle \exp(\boldsymbol{q} \cdot \Delta \boldsymbol{r}(\tau)) \rangle$ needs then to be evaluated numerically.

VI. Summary and conclusion

We have investigated theoretically and experimentally what is measured by DWS for composite systems mixing two types of scatterers having each a dynamical timescale. We have clearly identified conditions for a single decorrelation due to either one or the other scatterer, and a range of experimental conditions where both dynamics are decoupled and separated in time (leading to an intermediate plateau in the DWS curve).

From a general point of view, for a parallel slab filled with any type of liquid dispersion (like a foam or an emulsion) of transport mean free path $l^* \ll L$, the transport of light may be treated using diffusive transport approximation. The typical path length $s \sim L^2/2l^*$ must be compared to the scattering length l_c due to the colloidal particles. If $l_c \gg L^2/2l^*$, the scattering due to the colloidal particle is negligible; here, we have investigated the regime where $l_c \gtrapprox L^2/2l^*$, but note also that if $l_c \ll L^2/2l^*$ we have another regime, with multiple scattering on colloidal particles. Note that this scattering regime may be achieved with $l_c \gg l^*$, *i.e.* with no modification of the static scattering properties.

The analysis of the data collected on our experimental model system (colloidal beads within a foam) clearly shows and definitively proves that the origin of this type of two-decay shape is due to the presence of these two identified dynamical processes (intrinsic rearrangements due to coarsening and particle Brownian motion within the continuous liquid phase). This implements and confirms our previous study made on particle-stabilized foams, where the ratio of the adsorbed and free particles inside the foam was not directly controlled, neither the particle size nor polydispersity. As in this new study, the particles are never adsorbed at bubble interfaces, one can be sure that considering processes associated with the possible jamming/unjamming of adsorbed particles is not relevant.

We want to emphasize that the non-trivial features reported and explained here are particularly important for food science: as already stated, food products are often complex mixtures where small scatterers are present and distributed within an emulsion or foam (or even more complex multiple dispersions[32]). When dealing with complex turbid materials and performing light correlation experiments like DWS, these new results show that one has to be aware that a single decorrelation process is not necessarily due to the most obvious mechanism, and that data analysis is not straightforward. In particular, regarding the fact that even a low amount of colloids can dominate the dynamic scattering properties, the presence of uncontrolled impurities can easily and unfortunately be the dominant effect. In that respect, we also show here that adjusting the setup conditions or the dispersion parameters can be a way to tune the length scales and to separate the dynamics.

For such a composite system, we have developed a generic theoretical framework, and we have shown that despite some agreement, there are still some remaining questions: this opens interesting fundamental questions about the optics of fast scatterers in a slowly evolving matrix, and possibly about the effect of confinement on the Brownian motion. Once the origins of the limits of model will be known, one could "invert the problem" and consider that an optical method could be developed for rapid and easy measuring of low amount or traces of scatterers in a transparent fluid: using the relatively simple setup of DWS and dispersing the solutions within a slowly evolving matrix should indeed be sufficient. Using a spatially resolved DWS setup,[53] the concentration field of colloidal particles should also be measurable.

References

1 See for example: *Soft and Fragile Matter*, ed. M. Cates and M. Evans, Institute of Physics Publishing, Bristol, 2000.
2 G. Maret and P. E. Wolf, *Z. Phys. B: Condens. Matter*, 1987, **65**, 409.
3 D. Pine, D. A. Weitz, P. M. Chaikin and E. Herbolzheimer, *Phys. Rev. Lett.*, 1988, **60**, 1134.
4 D. J. Pine, D. A. Weitz, P. E. Wolf, G. Maret, E. Herbolzheimer and P. M. Chaikin, in *Scattering and Localization of Classical Waves in Random Media*, ed. P. Sheng, World Scientific, 1990.
5 D. A. Weitz and D. J. Pine, *Dynamic Light Scattering: The Methods and Applications*, Oxford University Press, Oxford, 1993, p. 652.
6 X. L. Wu, D. J. Pine, P. M. Chaikin, J. S. Huang and D. A. Weitz, *J. Opt. Soc. Am. B*, 1990, **7**, 15.
7 D. J. Durian, D. A. Weitz and D. J. Pine, *Science*, 1991, **252**, 686.
8 D. J. Durian, D. A. Weitz and D. Pine, *Phys. Rev. A: At., Mol., Opt. Phys.*, 1991, **44**, R7902.
9 D. J. Durian, *Phys. Rev. E: Stat. Phys., Plasmas, Fluids, Relat. Interdiscip. Top.*, 1995, **51**, 3350.
10 P. A. Lemieux, M. U. Vera and D. J. Durian, *Phys. Rev. E: Stat. Phys., Plasmas, Fluids, Relat. Interdiscip. Top.*, 1998, **57**, 4498.
11 A. Knaebel, M. Bellour, J. P. Munch, V. Viasnoff, F. Lequeux and J. L. Harden, *Europhys. Lett.*, 2000, **52**, 73.
12 F. Scheffold, S. E. Skipetrov, S. Romer and P. Schurtenberger, *Phys. Rev. E: Stat. Phys., Plasmas, Fluids, Relat. Interdiscip. Top.*, 2001, **63**, 061404.
13 R. Bandyopadhyay, A. S. Gittings, S. S. Suh, P. K. Dixon and D. J. Durian, *Rev. Sci. Instrum.*, 2005, **76**, 093110.
14 L. Cipelletti, H. Bissig, V. Trappe, P. Ballesta and S. Mazoyer, *J. Phys.: Condens. Matter*, 2003, **15**, S257.
15 A. D. Gopal and D. J. Durian, *J. Opt. Soc. Am. A*, 1997, **14**, 150.
16 P. Hebraud, F. Lequeux, J. P. Munch and D. Pine, *Phys. Rev. Lett.*, 1997, **78**, 4657.
17 A. D. Gopal and D. J. Durian, *J. Colloid Interface Sci.*, 1999, **213**, 169.
18 S. Cohen-addad and R. Hohler, *Phys. Rev. Lett.*, 2001, **86**, 4700.
19 A. D. Gopal and D. J. Durian, *Phys. Rev. Lett.*, 2003, **91**, 188303-1.
20 S. Cohen-addad, R. Hohler and Y. Khidas, *Phys. Rev. Lett.*, 2004, **93**, 028302-1.
21 S. Marze, D. Langevin and A. Saint-Jalmes, *J. Rheol.*, 2008, **52**, 1091.
22 Y. Hemar, D. N. Pinder, R. J. Hunter, H. Singh, P. Hebraud and D. S. Horne, *J. Colloid Interface Sci.*, 2003, **264**, 502.
23 M. Alexander and D. G. Dalgleish, *Curr. Opin. Colloid Interface Sci.*, 2007, **12**, 179.
24 M. Corredig and M. Alexander, *Trends Food Sci. Technol.*, 2008, **19**, 67.
25 R. Mezzenga, P. Schurtenberger, A. Burbridge and M. Michel, *Nat. Mater.*, 2005, **4**, 729.
26 Y. Hemar and D. S. Horne, *Colloids Surf., B*, 1999, **12**, 239.
27 E. TenGrotenhuis, M. Paques and E. VanDerLinden, *J. Colloid Interface Sci.*, 2000, **227**, 495.
28 H. M. Wyss, S. Romer, F. Scheffold, P. Schurtenberger and L. J. Glaucker, *J. Colloid Interface Sci.*, 2001, **240**, 89.
29 C. Eliot, D. S. Horne and E. Dickinson, *Food Hydrocolloids*, 2005, **19**, 279.
30 H. G. M. Ruis, K. Van Gruijthuijsen, P. Venema and E. VanDerLinden, *Langmuir*, 2007, **23**, 1007.
31 H. G. M. Ruis, P. Venema and E. VanDerLinden, *Langmuir*, 2008, **24**, 7117.
32 R. Vincent, G. Gillies and A. Stratner, *Soft Matter*, 2011, **7**, 2697.
33 U. Pickering, *J. Chem. Soc. Trans.*, 1907, **91**, 2001.
34 S. Arditty, C. P. Whitby, B. P. Binks, V. Schmitt and F. Leal-Calderon, *J. Colloid Interface Sci.*, 2004, **275**, 659.
35 A. Stocco, J. Crassous, A. Salonen, A. Saint-Jalmes and D. Langevin, *Phys. Chem. Chem. Phys.*, 2011, **13**, 3064.
36 P. Snabre and J. Crassous, *Eur. Phys. J. E*, 2009, **29**, 149.
37 I. Flammer, G. Bucher and J. Rička, *J. Opt. Soc. Am. A*, 1998, **15**, 2066.
38 M. J. Stephen, *Phys. Rev. B: Condens. Matter Mater. Phys.*, 1988, **37**, 1.
39 M. U. Vera, A. Saint-Jalmes and D. J. Durian, *Appl. Opt.*, 2001, **40**, 4210.
40 R. Höhler and S. Cohen-Addad, *J. Phys.: Condens. Matter*, 2005, **17**, R1041.
41 A. Saint-Jalmes, *Soft Matter*, 2006, **2**, 836.
42 S. Cohen-addad, M. Krzan, R. Hohler and B. Herzhaft, *Phys. Rev. Lett.*, 2007, **99**, 168001.
43 B. P. Binks, *Curr. Opin. Colloid Interface Sci.*, 2002, **7**, 21.
44 J. W. Goodman, *Statistical Optics*, Wiley-Interscience, New York, 2000.
45 B. Berne and R. Pecora, *Dynamic Light Scattering: With Applications to Chemistry, Biology, and Physics*, Wiley, New York, 1976.
46 H. Hoballah, R. Hohler and S. Cohen-addad, *J. Phys. II*, 1997, **7**, 1215.
47 C. F. Bohrenand D. R. Huffman, *Absorption and Scattering of Light by Small Particles*, Wiley-Interscience, 1998.
48 A. S. Gittings, R. Bandyopadhyay and D. J. Durian, *Europhys. Lett.*, 2004, **65**, 414.
49 M. Schmiedeberg, M. F. Miri and H. Stark, *Eur. Phys. J. E*, 2005, **18**, 123.
50 Z. Sadjadi, M. Miri, M. R. Shaebani and S. Nakhaee, *Phys. Rev. E: Stat., Nonlinear, Soft Matter Phys.*, 2008, **78**, 031121.
51 J. Crassous, *Eur. Phys. J. E*, 2007, **23**, 145.
52 N. Louvet, O. Pitois and R. Hohler, *Phys. Rev. E: Stat., Nonlinear, Soft Matter Phys.*, 2010, **82**, 041405.
53 M. Erpelding, A. Amon and J. Crassous, *Phys. Rev. E: Stat., Nonlinear, Soft Matter Phys.*, 2008, **78**, 046104.